COMMUNICATION

ChemComm
www.rsc.org/chemcomm

Interdependence of redox state, hydrogen bonding, anion recognition and charge partition in crystals of (EDT-TTF-CONHMe)$_6$ [$Re_6Se_8(CN)_6$] (CH_3CN)$_2$(CH_2Cl_2)$_2$†

Stéphane A. Baudron,[a] Patrick Batail,*[a] Carme Rovira,[b] Enric Canadell[c] and Rodolphe Clérac[d]

[a] *Laboratoire Chimie Inorganique, Matériaux et Interfaces, FRE 2447 CNRS-Université d'Angers, Bat K, 2 Boulevard Lavoisier, 49045 Angers, France. E-mail: patrick.batail@univ-angers.fr*

[b] *Centre de Recerca en Química Teòrica, Parc Científic de Barcelona, Josep Samitier 1-5, 08028 Barcelona, Spain*

[c] *Institut de Ciènca de Materials de Barcelona (CSIC), Campus de la UAB, 08193 Bellaterra, Spain*

[d] *CRPP-CNRS UPR8641, Avenue du Dr A. Schweitzer, 33600 Pessac, France*

Received (in Cambridge, UK) 27th March 2003, Accepted 5th June 2003
First published as an Advance Article on the web 25th June 2003

Neutral π-conjugated molecules and their radical cations co-exist in [(EDT-TTF-CONHMe$^{+\cdot}$)$_4$(EDT-TTF-CONHMe^0)$_2$] [$Re_6Se_8(CN)_6$]$^{4-}$ (CH_3CN)$_2$(CH_2Cl_2)$_2$ whose crystal structure reveals that, upon one-electron oxidation, an activation of the N–H and C–H hydrogen bond donor ability is coupled to a deactivation of the hydrogen bond acceptor character of the carbonyl oxygen atom: this is expressed in the supramolecular hydrogen bond pattern and, ultimately, into charge localisation and partition in the solid state.

The redox control of intermolecular recognition is a matter of active research.[1] Amide-functionalized metallocenes have particularly received much attention for anion recognition,[2] a consequence of the enhancement of N–H hydrogen bond donor character upon oxidation in solution and in the solid-state.[3] We[4] and others[5] have showed that amide-functionalized tetrathiafulvalene (TTF) derivatives also display modulation of their donor/acceptor hydrogen bonding ability in solution. We report here on the title phase where the methylamide-appended ethylenedithio-tetrathiafulvalene molecules, EDT-TTF-CONHMe,[6] are found to co-exist in their neutral and oxidised forms, revealing an interdependence of the redox state and a modulation of the hydrogen bond donor/acceptor character of the π-donor, and show how this is expressed into charge partition in the solid state. This is further substantiated by calculations of charges and electrostatic potentials which allow for a coherent interpretation of both the molecular recognition and its supramolecular expression.

Electrocrystallization in an H-shaped cell at a constant current of 0.5 μA for 2 weeks of EDT-TTF-CONHMe (5 mg) in a CH_2Cl_2–CH_3CN (1 : 1, 12 mL) solution containing (PPh_4)$_4$[$Re_6Se_8(CN)_6$],[7] (25 mg) affords shiny black platelets whose formulation, [EDT-TTF-CONHMe]$_6$[$Re_6Se_8(CN)_6$] (CH_3CN)$_2$(CH_2Cl_2)$_2$ was obtained by determination of their crystal structure.‡ The unit cell contains three independent π-donor molecules, one-half rhenium cluster on an inversion centre, one molecule of acetonitrile and one molecule of dichloromethane. Careful analysis of the central TTF cores bond lengths indicates that among the three independent molecules, two, noted A and B, are radical cations and one, C, is neutral, as shown in Fig. 1. Hence, the novel formulation indicating charge localisation reads [($A^{+\cdot}$)$_2$($B^{+\cdot}$)$_2$(C^0)$_2$] [$Re_6Se_8(CN)_6$]$^{4-}$ (CH_3CN)$_2$(CH_2Cl_2)$_2$. At the organic–inorganic interface, a hydrogen bond network appears. This network is built out of $R_2^1(7)$ motifs as usually observed for EDT-TTF-CONHMe[6]. Although both $A^{+\cdot}$ and C^0 form this motif by capturing a nitrile of the rhenium cluster, note that, as observed previously in [EDT-TTF-CONHMe]$_2$[Cl, H_2O],[4] both N–H···N and C–H···N hydrogen bond lengths (Fig. 1) are shorter with $A^{+\cdot}$ than with C^0. This indicates that the N–H and C–H hydrogen bond donor character for $A^{+\cdot}$ is stronger than that for C^0. Meanwhile, it is remarkable that the C=O's of $A^{+\cdot}$ and $B^{+\cdot}$

† Electronic supplementary information (ESI) available: plot of magnetic susceptibility against temperature. See http://www.rsc.org/suppdata/cc/b3/b303416j/

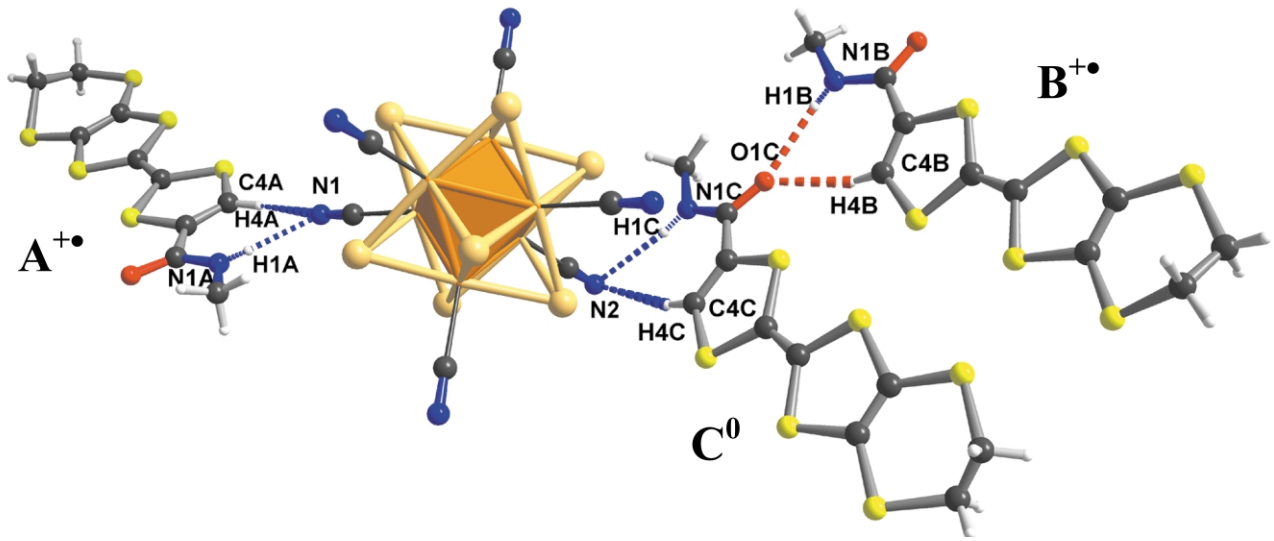

Fig. 1 Hydrogen bond network in [EDT-TTF-CONHMe]$_6$[$Re_6Se_8(CN)_6$] (CH_3CN)$_2$(CH_2Cl_2). Bond distances (D···A and H···A in Å) and angles (D–H···A in °): N_{1A}–H_{1A}···N_1, 2.869(9), 2.055, 157.8; C_{4A}–H_{4A}···N_1, 3.292(9), 2.402, 160.1; N_{1B}–H_{1B}···O_{1C}, 3.136(9), 2.286, 169.9; C_{4B}–H_{4B}···O_{1C}, 3.066(10), 2.203, 153.8; N_{1C}–H_{1C}···N_2, 3.156(10), 2.309, 168.3; C_{4C}–H_{4C}···N_2, 3.430(10), 2.523, 165.2.

DOI: 10.1039/b303416j

are not involved in any hydrogen bond in this salt. Instead, only the oxygen atom of neutral C^0 is grasped by a pair of hydrogen bond tweezers. Hence, upon oxidation of the conjugated redox system, an activation of the N–H and C–H hydrogen bond donor ability occurs and is coupled to a deactivation of the hydrogen bond acceptor character of the carbonyl oxygen atom, the latter paralleling Rotello's similar, albeit inverse, observation in flavins.[1b] Note that this result has to be distinguished from charge-assisted hydrogen bonding[8] where the charge is localised on the hydrogen bond donor/acceptor group (ammoniums, carboxylate...).

The electrostatic potentials for $A^{+\cdot}$, $B^{+\cdot}$ and C^0 have been evaluated by means of B3LYP-DFT//3-21G calculations.[9] The constant electrostatic potential surfaces for $A^{+\cdot}$ and C^0 (Fig. 2) clearly show the deactivation of the carbonyl oxygen and activation of the N–H and C–H hydrogen bonding abilities upon oxidation. The electrostatic potential of the carbonyl oxygen decreases from C^0 to $A^{+\cdot}$ (by 75.9 kcal mol^{-1}) and to $B^{+\cdot}$ (by 73.3) clearly showing the deactivation. At the same time, the electrostatic potential of the N–H (C–H) hydrogen decreases by 67.5 (84.1) and 68.8 (83.8) kcal mol^{-1} from C^0 to $A^{+\cdot}$ and $B^{+\cdot}$, respectively. Thus, the increase in the hydrogen bonding ability of N–H and C–H is slightly weaker for $A^{+\cdot}$. Analysis of the calculated charges for the oxygen and hydrogen atoms leads to exactly the same results.

Thus, the primary structural motif is $[B^{+\cdot}\cdots C^0]$ (Fig. 1) which satisfies both the strongest H-bond donors, *i.e.*, the activated protons N–H and C–H of radical cation $B^{+\cdot}$ and the strongest H-bond acceptor, *i.e.*, the oxygen atom of neutral C^0. Then, the second best pair of activated tweezers of radical cation $A^{+\cdot}$ goes for the second best H-bond acceptor, that is, one cluster cyanide, since the remaining two oxygen atoms are deactivated. Finally, the non-activated pair of tweezers of neutral C^0 is strong enough to bind another cyanide. Altogether, the former radical cations thus positioned at the organic–inorganic interface overlap and generate the two-dimensional pattern shown in Fig. 3. Note that the $A^{+\cdot}$ pairs are strongly dimerised whereas the $B^{+\cdot}$ pairs are considerably less. This observation is consistent with our analysis since by strongly interacting with C^0, $B^{+\cdot}$ is less free than $A^{+\cdot}$ to optimise stabilising π_{HOMO}–π_{HOMO} interactions. Thus, the weakly interacting $B^{+\cdot}$ donors are diluted and confined in a sea of diamagnetic, charged ($[A^{+\cdot}]_2$) or neutral (C^0) units. The observed temperature dependence of the spin susceptibility (Curie–Weiss behavior, $\theta \approx -10$ K) measured on one single crystal by EPR experiments (one single narrow resonance with $g_{max} = 2.013$ and $\Delta H_{max} = 17$ Oe) confirm the presence of essentially localised, weakly antiferromagnetically coupled spins, in sharp contrast with the metallic behaviour of the [EDT-TTF-CONHMe]$_2$[Cl, H_2O].[4] This makes clear the subtle interplay of stoichiometry, redox state, hydrogen bonding and π–π interactions in determining the structure and transport properties of molecular materials.

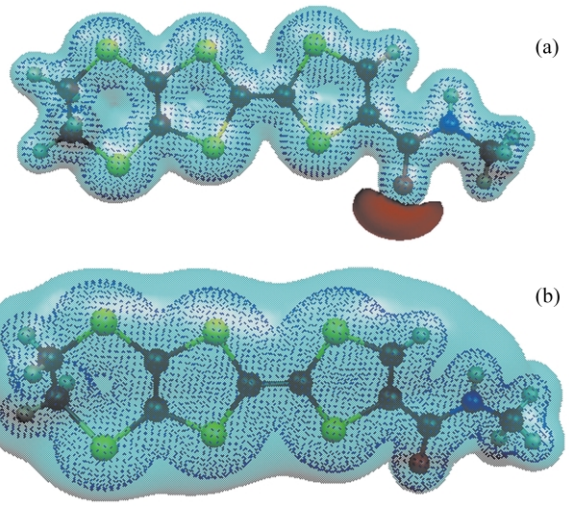

Fig. 2 Surfaces of constant electrostatic potential calculated for: (a) C^0 and (b) $A^{+\cdot}$. Values of the electrostatic potential are −44 kcal mol^{-1} (red), +94 kcal mol^{-1} (light blue) and +188 kcal mol^{-1} (blue dots).

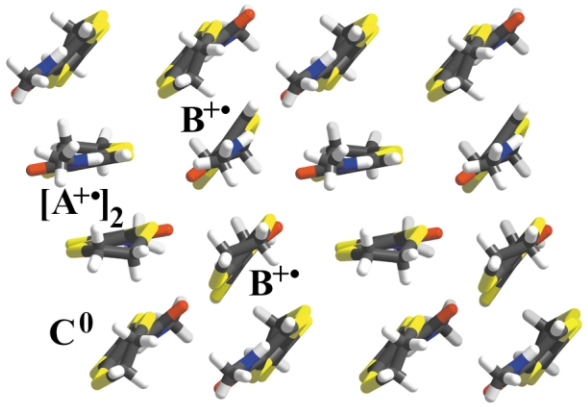

Fig. 3 Rows of neutral molecules C^0 confine fully oxidised, diamagnetic dimers, $[A^{+\cdot}]_2$ and pairs of essentially discrete, paramagnetic $B^{+\cdot}$.

This work was supported by the CNRS and the Région Pays de la Loire (joint PhD grant to S.A.B.), DGI-Spain (Projects BFM2000-1312-C02-01 and BQU2002-04587-CO02), Generalitat de Catalunya (2001 SGR 333 and 044) and CNRS-CSIC (2002-2003 11432). C. R. acknowledges financial support of the "Ramón y Cajal"; program of the Spanish MCYT.

Notes and references

‡ *Crystal structure analysis* for [EDT-TTF-CONHMe]$_6$[$Re_6Se_8(CN)_6$][CH_3CN]$_2$(CH_2Cl_2)$_2$:$C_{72}H_{64}Cl_4N_{14}O_6Re_6S_{36}Se_8$, triclinic, space group *P*1, a = 12.1696(10), b = 12.7211(11). c = 18.8992(16) Å, α = 94.672(10), β = 98.494(10), γ = 95.591(10)°, V = 2867.5(4) Å^3, D_c = 2.459 g cm^{-3}, Z = 1. Black plate-like crystal (0.46 × 0.28 × 0.04 mm). Data were collected on a STOE Imaging Plate diffractometer (IPDS) with Mo–Kα radiation, λ = 0.71073 Å at 150(2) K. A total of 34554 reflections were collected up to θ = 27.9° of which 12861 are independent among 8089 observed [$F_o^2 > 2\sigma(F_o^2)$]. The structure solution (SHELXS-97) and refinements on F_o^2 (SHELXL-97) gave R(obs) = 0.0333 [R(all) = 0.0641] and R_w(obs) = 0.0617 [R_w(all) = 0.0678] for 672 parameters ; min and max residual electron densities were −1.89 and 1.73 e Å^{-3}. CCDC 207256. See http://www.rsc.org/suppdata/cc/b3/b303416j/ for crystallographic data in .cif format.

1 (*a*) P. L. Boulas, M. Gomez-Kaifer and L. Echegoyen, *Angew. Chem., Int. Ed.*, 1998, **37**, 216; (*b*) A. Niemz and V. M. Rotello, *Acc. Chem. Res.*, 1999, **32**, 44; (*c*) A. E. Kaifer, *Acc. Chem. Res.*, 1999, **32**, 62; (*d*) J. H. R. Tucker and S. R. Collinson, *Chem. Soc. Rev.*, 2002, **31**, 147.
2 P. D. Beer and P. A. Gale, *Angew. Chem., Int. Ed.*, 2001, **40**, 486.
3 J. D. Carr, S. J. Coles, M. B. Hursthouse, M. E. Light, J. H. R. Tucker and J. Westwood, *Angew. Chem., Int. Ed.*, 2000, **39**, 3296.
4 K. Heuzé, C. Mézière, M. Fourmigué, P. Batail, C. Coulon, E. Canadell, P. Auban-Senzier and D. Jérome, *Chem. Mater.*, 2000, **12**, 1898.
5 L. M. Goldenberg and O. Neilands, *J. Electroanal. Chem.*, 1999, **463**, 212; A. S. F. Boyd, G. Cooke, F. M. A. Duclairoir and V. M. Rotello, *Tetrahedron Lett.*, 2003, **44**, 303.
6 K. Heuzé, M. Fourmigué and P. Batail, *J. Mater. Chem.*, 1999, **9**, 2373.
7 T. Yoshimura, S. Ishizaka, Y. Sasaki, H.-B. Kim, N. Kitamura, N. G. Naumov, M. N. Sokolov and V. E. Fedorov, *Chem. Lett.*, 1999, 1121.
8 D. Braga and F. Grepioni, *Acc. Chem. Res.*, 2000, **33**, 601.
9 M. J. Frisch, G. W. Trucks, H. B. Schlegel, G. E. Scuseria, M. A. Robb, J. R. Cheeseman, V. G. Zakrzewski, J. A. Montgomery, Jr., R. E. Stratmann, J. C. Burant, S. Dapprich, J. M. Millam, A. D. Daniels, K. N. Kudin, M. C. Strain, O. Farkas, J. Tomasi, V. Barone, M. Cossi, R. Cammi, B. Mennucci, C. Pomelli, C. Adamo, S. Clifford, J. Ochterski, G. A. Petersson, P. Y. Ayala, Q. Cui, K. Morokuma, D. K. Malick, A. D. Rabuck, K. Raghavachari, J. B. Foresman, J. Cioslowski, J. V. Ortiz, B. B. Stefanov, G. Liu, A. Liashenko, P. Piskorz, I. Komaromi, R. Gomperts, R. L. Martin, D. J. Fox, T. Keith, M. A. Al-Laham, C. Y. Peng, A. Nanayakkara, C. Gonzalez, M. Challacombe, P. M. W. Gill, B. G. Johnson, W. Chen, M. W. Wong, J. L. Andres, M. Head-Gordon, E. S. Replogle and J. A. Pople, *GAUSSIAN 98 (Revision A.7)*, Gaussian, Inc., Pittsburgh, PA, 1998.